Macromolecules

Article

pubs.acs.org/Macromolecules

Preparation and Cross-Linking of All-Acrylamide Diblock Copolymer Nano-Objects via Polymerization-Induced Self-Assembly in Aqueous Solution

Sarah J. Byard,[†] Mark Williams,[†] Beulah E. McKenzie,[†] Adam Blanazs,[‡] and Steven P. Armes*[,†]

[†]Department of Chemistry, University of Sheffield, Brook Hill, Sheffield, South Yorkshire S3 7HF, U.K.

[‡]BASF SE, GMV/P-B001, 67056 Ludwigshafen, Germany

Supporting Information

ABSTRACT: Various carboxylic acid-functionalized poly(*N*,*N*-dimethylacrylamide) (PDMAC) macromolecular chain transfer agents (macro-CTAs) were chain-extended with diacetone acrylamide (DAAM) by reversible addition−fragmentation chain transfer (RAFT) aqueous dispersion polymerization at 70 °C and 20% w/w solids to produce a series of PDMAC−PDAAM diblock copolymer nano-objects via polymerization-induced self-assembly (PISA). TEM studies indicate that a PDMAC macro-CTA with a mean degree of polymerization (DP) of 68 or higher results in the formation of well-defined spherical nanoparticles with mean diameters ranging from 40 to 150 nm. In contrast, either highly anisotropic worms or polydisperse vesicles are formed when relatively short macro-CTAs (DP = 40−58) are used. A phase diagram was constructed to enable accurate targeting of pure copolymer morphologies. Dynamic light scattering (DLS) and aqueous electrophoresis studies indicated that in most cases these PDMAC−PDAAM nano-objects are surprisingly resistant to changes in either solution pH or temperature. However, $PDMAC_{40}$−$PDAAM_{99}$ worms do undergo partial dissociation to form a mixture of relatively short worms and spheres on adjusting the solution pH from pH 2−3 to around pH 9 at 20 °C. Moreover, a change in copolymer morphology from worms to a mixture of short worms and vesicles was observed by DLS and TEM on heating this worm dispersion to 50 °C. Postpolymerization cross-linking of concentrated aqueous dispersions of PDMAC−PDAAM spheres, worms, or vesicles was performed at ambient temperature using adipic acid dihydrazide (ADH), which reacts with the hydrophobic ketone-functionalized PDAAM chains. The formation of hydrazone groups was monitored by FT-IR spectroscopy and afforded covalently stabilized nano-objects that remained intact on exposure to methanol, which is a good solvent for both blocks. Rheological studies indicated that the cross-linked worms formed a stronger gel compared to linear precursor worms.

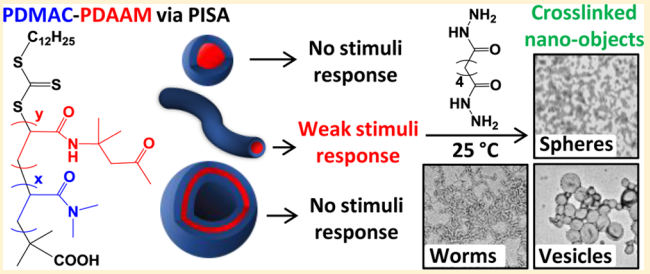

INTRODUCTION

AB diblock copolymer self-assembly has attracted considerable attention in recent decades as a convenient method for preparing organic nanoparticles with spherical, wormlike, or vesicular morphologies.[1−10] Traditionally, block copolymer self-assembly is achieved using a postpolymerization processing method such as a solvent switch.[5,7−9,11,12] However, this approach typically requires relatively low copolymer concentrations (<1%), which makes many potential commercial applications economically unviable.

Over the past decade, polymerization-induced self-assembly (PISA) has been used to produce well-defined AB diblock copolymer nanoparticles at high solids (10−50% w/w).[13−20] Successful PISA requires a controlled/living polymerization technique such as reversible addition−fragmentation chain transfer (RAFT) polymerization which provides polymers with low dispersities and predictable mean degrees of polymerization (DP). *In situ* self-assembly occurs during polymerization when a soluble macromolecular chain transfer agent (macro-CTA) is extended with a second monomer that forms an insoluble block. In principle, if appropriate monomers are selected, then PISA can be conducted in any solvent.[21,22] In practice, PISA syntheses in aqueous media are particularly attractive from an environmental perspective,[23] and such diblock copolymer nano-objects can lead directly to potential biomedical applications.[15,24−26]

Successful PISA formulations based on RAFT aqueous dispersion polymerization[20,26−36] and RAFT aqueous emulsion polymerization[13,16,17,19,37−44] have been reported. However, RAFT aqueous emulsion polymerization typically results in kinetically trapped spherical nanoparticles,[13,37,40,42−46] with rather few literature examples of worms or vesicles being accessed using such formulations.[16,38,39,41,47,48] On the other hand, RAFT aqueous dispersion polymerization usually allows straightforward access to such "higher order" morphologies.[14,20,23,28,33,49−51]

Received: December 9, 2016
Revised: February 1, 2017
Published: February 14, 2017

DOI: 10.1021/acs.macromol.6b02643
Macromolecules 2017, 50, 1482−1493

An essential prerequisite for aqueous dispersion polymerization is a water-miscible monomer that polymerizes to produce a water-insoluble polymer. Cia and co-workers reported successful PISA syntheses via RAFT aqueous dispersion polymerization of a cationic core-forming monomer, 2-aminoethylacrylamide hydrochloride, in the presence of an anionic polyelectrolyte, which induces *in situ* polyion complexation.[52] However, it is much more common to use nonionic monomers such as 2-hydroxypropyl methacrylate, *N*-isopropylacrylamide, *N*,*N*-diethylacrylamide, 2-methoxyethyl acrylate, or di(ethylene glycol) methyl ether methacrylate. Recently, a sixth nonionic monomer, diacetone acrylamide (DAAM), has been explored in the context of RAFT aqueous dispersion polymerization.[51,53−55] DAAM is highly water soluble and forms a water-insoluble homopolymer at a mean degree of polymerization (DP) as low as 50.[53]

DAAM enables ketone groups to be conveniently introduced for postpolymerization functionalization.[56−60] Recently, DAAM has been utilized as the core-forming block in PISA formulations. For example, Jiang et al. prepared spherical nanoparticles by chain-extending a poly(2-hydroxypropyl methacrylamide) macro-CTA with DAAM.[53] Replacing small amounts of DAAM with *N*-2-aminoethylacrylamide hydrochloride produced primary amine-functionalized nanoparticles that could be core-cross-linked using Schiff base chemistry.[53]

An and co-workers reported the formation of well-defined nano-objects using a poly(*N*,*N*-dimethylacrylamide) (PDMAC) macro-CTA.[51] Both PDMAC−PDAAM spheres and vesicles could be fluorescently labeled by reacting fluorescein-5-thiosemicarbazide with the ketone moiety in the DAAM residues. The same team prepared vesicles via the RAFT aqueous dispersion copolymerization of DAAM with allyl acrylamide using a PDMAC macro-CTA. Comparable acrylamide comonomer reactivities enabled vesicle formation via PISA, followed by latent cross-linking within the vesicle membranes via the less reactive pendent allyl groups.[54]

Recently, Gao et al. reported the formation of higher-order structures such as pore-switchable *nanotubes* by chain extension of a poly(2-hydroxypropyl methacrylamide) macro-CTA with DAAM at high solids (>35%).[55] These workers attribute the formation of these unusual higher-order nano-objects to hydrogen bonding. However, as far as we are aware, there are as yet no reports of PDAAM-based block copolymer *worms*. This omission is perhaps not too surprising because numerous PISA studies have shown that worms typically occupy a relatively narrow phase space.[33,61,62] Given the literature precedent with other core-forming blocks such as poly(2-hydroxypropyl methacrylate) (PHPMA), poly(*N*-isopropylacrylamide) (PNIPAM), and poly(2-methoxyethyl acrylate) (PMEA),[18,29,63−65] if such PDAAM-based worms could be obtained then stimulus-responsive behavior might be anticipated as a result of variable hydration of the core-forming chains and/or ionization of terminal carboxylic acid groups on the stabilizer block.[63,66]

Blanazs et al. monitored the evolution of copolymer morphology during the PISA synthesis of $PGMA_{47}$−$PHPMA_{200}$ diblock copolymer nano-objects using TEM.[27] The worm phase was shown to be one of several intermediate states between spheres and vesicles. Similar findings have been reported for other PISA formulations, suggesting that this is generic behavior.[28,61,67] Thus, if both spheres and vesicles can be produced using a PDMAC−PDAAM PISA formulation, worms should also be accessible if appropriate conditions can be identified.

Moreover, the ketone moiety within the DAAM residues has not yet been exploited for covalent stabilization of diblock copolymer nano-objects. Typically, cross-linking is achieved via the addition of a bifunctional vinyl monomer such as ethylene glycol dimethacrylate (EGDMA) to form a third hydrophobic block.[18,49,68−70] This approach works well for spheres and vesicles but can be problematic for the worm phase.[68] This is because even minor perturbations to the copolymer composition can lead to the formation of mixed phases (e.g., worms plus spheres or worms plus vesicles).

Herein we utilize RAFT aqueous dispersion polymerization to prepare a series of PDMAC−PDAAM diblock copolymer nano-objects. The mean DPs of the PDMAC stabilizer block and the PDAAM core-forming block have been systematically varied to produce well-defined spheres, worms and vesicles at 20% w/w solids, and a phase diagram has been constructed to facilitate reproducible syntheses of such pure phases. Moreover, we examine whether the worms exhibit either thermoresponsive or pH-responsive behavior. Finally, the cross-linking of such nano-objects is explored via postpolymerization modification using a commercial water-soluble adipic acid dihydrazide (ADH) reagent at ambient temperature.

EXPERIMENTAL SECTION

Materials. 2-(Dodecylthiocarbonothioylthio)-2-methylpropionic acid (DDMAT), *N*,*N*-dimethylacrylamide (DMAC), and 2,2′-azobis(2-methylpropionitrile) (AIBN) were purchased from Sigma-Aldrich and used as received. Diacetone acrylamide (DAAM), adipic acid dihydrazide (ADH), and 4,4′-azobis(4-cyanovaleric acid) (ACVA) were purchased from Alfa Aesar and were used as received. Deuterated methanol was purchased from Cambridge Isotope Laboratories. Dioxane was purchased from Sigma-Aldrich UK, and diethyl ether was purchased from Fisher Scientific. All solvents were HPLC grade.

Polymer Characterization. *^{1}H NMR Spectroscopy.* All NMR spectra were recorded using a 400 MHz Bruker Avance III HD 400 spectrometer in deuterated methanol at 25 °C (64 scans were required to ensure high-quality spectra).

UV−Vis Absorption Spectroscopy. UV−vis absorption spectra were recorded between 200 and 800 nm using a PC-controlled UV-1800 spectrophotometer at 25 °C using a 1 cm path length quartz cell. A Beer−Lambert curve was constructed using a series of ten DDMAT solutions in methanol. The absorption maximum at 311 nm assigned to the trithiocarbonate group[71] was used for this calibration plot, and DDMAT concentrations were selected such that the absorbance always remained below unity. The mean DP for each of the five macro-CTAs was determined using the molar extinction coefficient of 16 300 ± 160 mol^{-1} dm^3 cm^{-1} determined for the DDMAT.

Gel Permeation Chromatography (GPC). Copolymer molecular weight distributions were assessed using DMF GPC. The setup was comprised of two Agilent PL gel 5 μm Mixed-C columns and a guard column connected in series to an Agilent 1260 Infinity GPC system equipped with both refractive index and UV−vis detectors (only the refractive index detector used) operating at 60 °C. The GPC eluent was HPLC-grade DMF containing 10 mM LiBr at a flow rate of 1.0 mL min^{-1}. DMSO was used as a flow-rate marker. Calibration was achieved using a series of ten near-monodisperse poly(methyl methacrylate) standards (ranging in M_p from 625 to 618 000 g mol^{-1}). Chromatograms were analyzed using Agilent GPC/SEC software.

Dynamic Light Scattering (DLS). The intensity-average sphere-equivalent diameter of diblock copolymer nano-objects was determined at 25 °C by DLS using a Malvern Zetasizer NanoZS instrument via the Stokes−Einstein equation, which assumes perfectly monodisperse, noninteracting spheres. All measurements were made on 0.1% w/w copolymer dispersions in either acidic aqueous solution

DOI: 10.1021/acs.macromol.6b02643
Macromolecules 2017, 50, 1482−1493

(pH 2.5) or methanol using disposable plastic cuvettes. Data were averaged over three consecutive runs. For variable temperature DLS studies, 0.1% w/w aqueous copolymer dispersions were heated from 5 to 50 °C, followed by cooling to 25 °C, at 5 °C intervals allowing 15 min for thermal equilibrium at each temperature. In this case, copolymer dispersions were analyzed using a glass cuvette, and data were averaged over three consecutive runs at each temperature.

Aqueous Electrophoresis. Zeta potential measurements were performed using a Malvern Zetasizer Nano ZS instrument on 0.1% w/w aqueous copolymer dispersions at 25 °C in the presence of 1 mM KCl. The initial copolymer dispersion was acidic (pH 2.5) with the solution pH being adjusted by addition of dilute NaOH, with 5 min being allowed for equilibrium at each pH. Zeta potentials were calculated from the Henry equation using the Smoluchowski approximation. Hydrodynamic DLS diameters were also recorded during these pH experiments. All data were averaged over three consecutive runs.

Transmission Electron Microscopy (TEM). Copper/palladium TEM grids (Agar Scientific, UK) were coated in-house to yield a thin film of amorphous carbon. The grids were then subjected to a glow discharge for 30 s. Individual 10.0 μL droplets of 0.1% w/w aqueous copolymer dispersions were placed on freshly treated grids for 1 min and then carefully blotted with filter paper to remove excess solution. To ensure sufficient electron contrast, uranyl formate (9.0 μL of a 0.75% w/w solution) was absorbed onto the sample-loaded grid for 20 s and then carefully blotted to remove excess stain. Each grid was then dried using a vacuum hose. Imaging was performed using a FEI Tecnai Spirit 2 microscope fitted with an Orius SC1000B camera operating at 80 kV.

Rheology. An AR-G2 rheometer equipped with a variable temperature Peltier plate and a 40 mL 2° aluminum cone was used for all experiments. Percentage strain sweeps were conducted at 25 °C using a fixed angular frequency of 1.0 rad s^{-1}. Angular frequency sweeps were conducted at 25 °C using a constant percentage strain of 1.0%.

FT-IR Spectroscopy. FT-IR spectra were recorded for solid samples using a Thermo Scientific Nicolet iS10 FT-IR spectrometer fitted with a Golden Gate Diamond ATR accessory. Each spectrum was averaged over 500 scans at a resolution of 4 cm^{-1}.

Synthesis of Poly(N,N-dimethylacrylamide) (PDMAC) Macro-CTAs via RAFT Solution Polymerization. A typical protocol for the synthesis of a $PDMAC_{68}$ macro-CTA was conducted as follows. 2-(Dodecylthiocarbonothioylthio)-2-methylpropionic acid (DDMAT) (0.613 g, 1.68 mmol), AIBN (27.0 mg 0.17 mmol, CTA/AIBN molar ratio = 10.0), and DMAC (10.0 g, 0.101 mol) were weighed into a 100 mL round-bottomed flask. Dioxane (24.8 mL) was added to produce a 30% w/w solution, which was purged with nitrogen for 30 min. The sealed flask was immersed into an oil bath set at 70 °C for 25 min (final DMAC conversion = 89%, as judged by ^{1}H NMR spectroscopy), and the polymerization was subsequently quenched by immersing the flask in ice, followed by exposure to air. Dioxane (50 mL) was added to the reaction solution, followed by precipitation into a 10-fold excess of diethyl ether (1 L). The precipitate was redissolved in dioxane and precipitated once more into excess diethyl ether. The crude macro-CTA was dissolved in deionized water, any residual diethyl ether/dioxane was removed under reduced pressure, and the resulting aqueous solution was freeze-dried for 48 h. The purified PDMAC macro-CTA was obtained as a yellow solid. End-group analysis using UV spectroscopy indicated a mean degree of polymerization of 68, and the M_n and M_w/M_n were 5700 g mol^{-1} and 1.12, respectively, as judged by DMF GPC. The same protocol was used to synthesize a $PDMAC_{40}$ macro-CTA, which had an M_n and M_w/M_n of 3200 g mol^{-1} and 1.12, a $PDMAC_{46}$ macro-CTA with an M_n and M_w/M_n of 4600 g mol^{-1} and 1.09, a $PDMAC_{58}$ macro-CTA with an M_n and M_w/M_n of 5100 g mol^{-1} and 1.09, and a $PDMAC_{77}$ macro-CTA with an M_n and M_w/M_n of 7100 g mol^{-1} and 1.11.

Synthesis of $PDMAC_{58}$–$PDAAM_{230}$ Diblock Copolymer Vesicles by RAFT Aqueous Dispersion Polymerization at pH 2.5. The typical protocol for the synthesis of $PDMAC_{58}$–$PDAAM_{230}$ vesicles at 20% w/w solids was as follows. $PDMAC_{58}$ macro-CTA (0.136 g, 0.022 mmol), ACVA (0.6 mg, 0.002 mmol, CTA/ACVA molar ratio = 10), and DAAM monomer (0.864 g, 5.1 mmol; target DP = 230) were weighed into a 14 mL vial. Deionized water adjusted to pH 2.5 with HCl (4.0 mL) was then added to give a 20% w/w aqueous solution, which was degassed for 15 min at 4 °C prior to immersion in an oil bath set at 70 °C. This reaction solution was stirred for 4 h and then quenched by exposure to air. The DAAM monomer conversion was greater than 98% as judged by ^{1}H NMR spectroscopy, while the M_n and M_w/M_n were 27 100 g mol^{-1} and 1.54, respectively, as judged by DMF GPC. All other PISA syntheses were conducted at the same initial volume (5.0 mL) at 20% w/w solids.

Postpolymerization Cross-Linking Using ADH. A typical protocol for cross-linking $PDMAC_{58}$–$PDAAM_{230}$ vesicles is as follows. A 20% w/w aqueous dispersion of $PDMAC_{58}$–$PDAAM_{230}$ vesicles (2.5 g) prepared using the previously stated protocol and adipic acid dihydrazide (ADH; 0.045 g, 0.26 mmol, DAAM/ADH molar ratio = 10.0) were added to a 14 mL vial. The reaction solution was stirred at 25 °C for 6 h.

RESULTS AND DISCUSSION

Homopolymerization of DMAC. The RAFT solution polymerization of DMAC in dioxane at 70 °C using 2-(dodecylthiocarbonothioylthio)-2-methylpropionic acid (DDMAT) as a CTA is outlined in Scheme 1. This water-soluble homopolymer precursor was chain-extended with DAAM via RAFT aqueous dispersion polymerization at 70 °C and 20% w/w solids. A kinetic study of the synthesis of

Scheme 1. Reaction Scheme for the Synthesis of DDMAT–$PDMAC_x$ Macro-CTA by RAFT Solution Polymerization of DMAC Using a DDMAT Chain Transfer Agent and Its Subsequent Chain Extension with DAAM via RAFT Aqueous Dispersion Polymerization at pH 2.5 To Produce $PDMAC_x$–$PDAAM_y$ Diblock Copolymer Nano-Objects

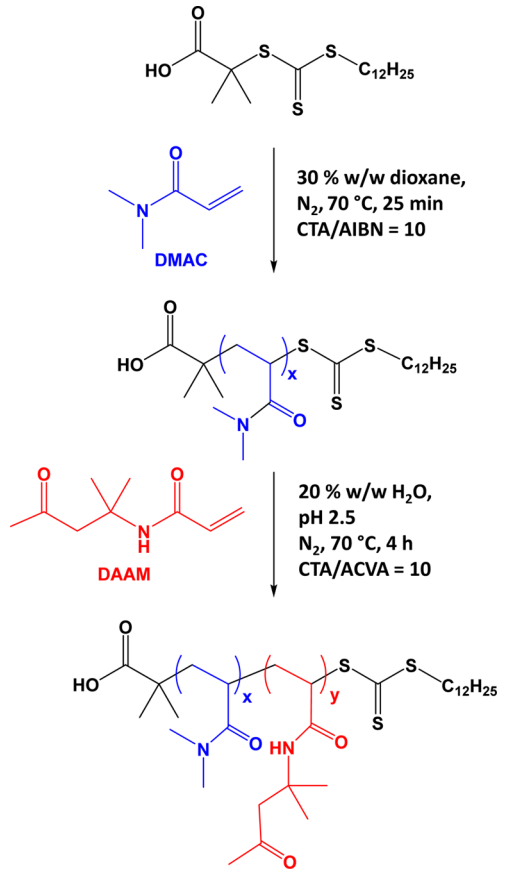

DOI: 10.1021/acs.macromol.6b02643
Macromolecules 2017, 50, 1482–1493

DDMAT−PDMAC$_{100}$ showed that the DMAC polymerization proceeded to ~98% conversion within 90 min (see Figure 1a).

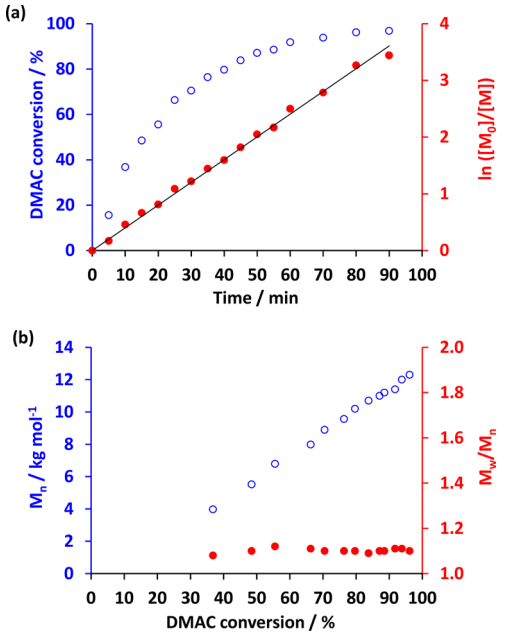

Figure 1. (a) DMAC conversion vs time plot and corresponding semilogarithmic plot and (b) evolution of number-average molecular weight (M_n) and dispersity (M_w/M_n) vs DMAC conversion for the RAFT solution polymerization of DMAC using a DDMAT chain transfer agent at 30% w/w in dioxane at 70 °C Conditions: DDMAT/AIBN molar ratio = 10 when targeting a DMAC/DDMAT molar ratio of 100. GPC analyses were performed in DMF eluent using a series of near-monodisperse poly(methyl methacrylate) calibration standards.

Monomer conversions were calculated from ^{1}H NMR spectra by comparing the integrated DMAC vinyl signals between 5.5 and 7 ppm to the combined polymer/monomer signals in the region between 2.3 and 3.25 ppm (Figure 2). A linear semilogarithmic plot indicated first-order kinetics with respect to DMAC (see Figure 1a). The linear evolution of M_n (DMF GPC vs PMMA standards) with conversion was accompanied by low dispersities throughout ($M_w/M_n \leq 1.12$), which indicates a well-controlled RAFT polymerization (see Figure 1b).[72−74] Subsequently, a range of PDMAC macro-CTAs were prepared with mean degree of polymerizations of 40, 46 58, 68, or 77, as determined by end-group analysis using UV spectroscopy (see Figure S1 for a typical Beer−Lambert plot obtained for DDMAT at its absorption maximum of 311 nm). GPC analysis indicated low dispersities (M_w/M_n = 1.09−1.12) for all five PDMAC macro-CTAs used in this work. Characterization data for these macro-CTAs are summarized in Table 1.

RAFT Aqueous Dispersion Polymerization of DAAM. Chain extension of the PDMAC macro-CTAs was conducted via RAFT aqueous dispersion polymerization of DAAM at 70 °C and 20% w/w solids (see Scheme 1). Recently, Lovett and co-workers have shown that ionization of CTA-derived carboxylic acid end groups can influence the copolymer morphology of diblock copolymer nano-objects prepared via PISA.[63,66] Thus, HCl was used to lower the solution pH to pH 2.5 so as to ensure that the terminal carboxylic acid groups located on the PDMAC stabilizer chains remained in their neutral acid form during the PISA synthesis. A kinetic study of the chain extension of PDMAC$_{58}$ with DAAM when targeting a DP of 120 for the core-forming block confirmed that ~99% conversion was obtained within 90 min (see Figure 3a). DAAM conversions were determined by comparison of the residual vinyl signals at 5.4−6.4 ppm to the PDAAM methyl signal

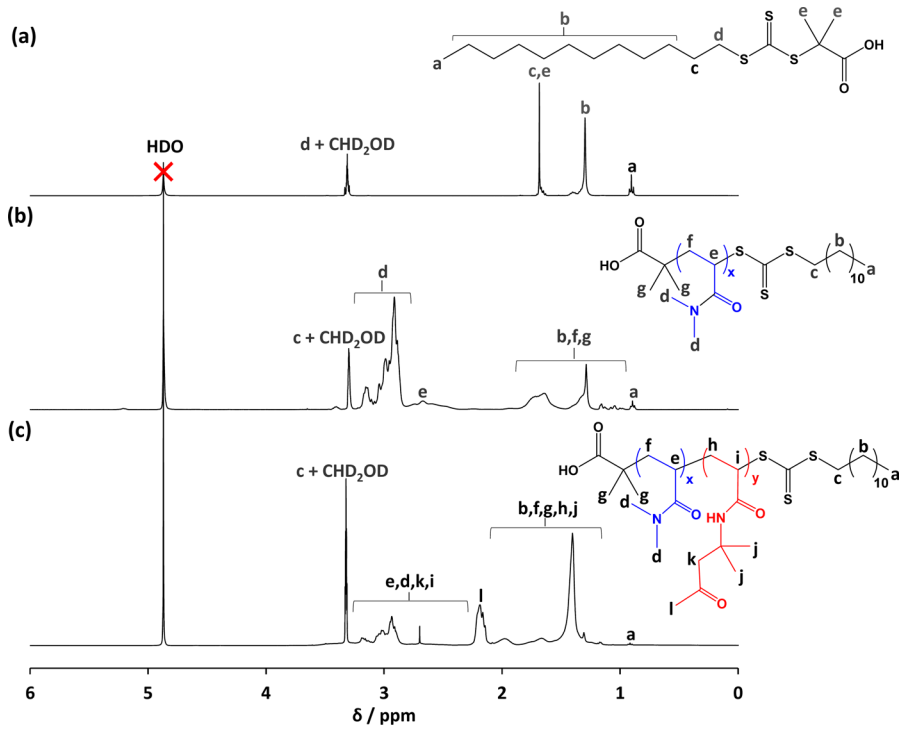

Figure 2. ^{1}H NMR spectra recorded in CD_3OD for (a) the DDMAT RAFT CTA used in this work, (b) a DDMAT−PDMAC$_{40}$ macro-CTA (see entry 1 in Table 1), and (c) a DDMAT−PDMAC$_{40}$−PDAAM$_{85}$ diblock copolymer (see entry 3 in Table S1).

DOI: 10.1021/acs.macromol.6b02643
Macromolecules 2017, 50, 1482−1493

Table 1. Summary of Conversion and Molecular Weight Data Obtained for PDMAC Macro-CTAs Prepared via RAFT Solution Polymerization of DMAC at 30% w/w in Dioxane at 70 °C

entry	macro-CTA	target DP	DMAC conv[a] (%)	actual DP[b]	$M_{n,th}$[c] (g mol^{-1})	$M_{n,GPC}$[d] (g mol^{-1})	M_w/M_n[d]
1	$PDMAC_{40}$	60	60	40	3900	3200	1.12
2	$PDMAC_{46}$	55	87	46	5100	4600	1.09
3	$PDMAC_{58}$	50	96	58	5100	5100	1.09
4	$PDMAC_{68}$	60	95	68	6000	5700	1.12
5	$PDMAC_{77}$	70	93	77	6800	7100	1.11

[a] ^{1}H NMR spectroscopy in CD_3OD. [b] UV spectroscopy analysis in methanol. [c] $M_{n,th} = (([DMAC]_0/[DDMAT]_0) \times DMAC\ conv \times M_{DMAC}) + M_{DDMAT}$. [d] Determined by DMF GPC using a series of near-monodisperse poly(methyl methacrylate) calibration standards.

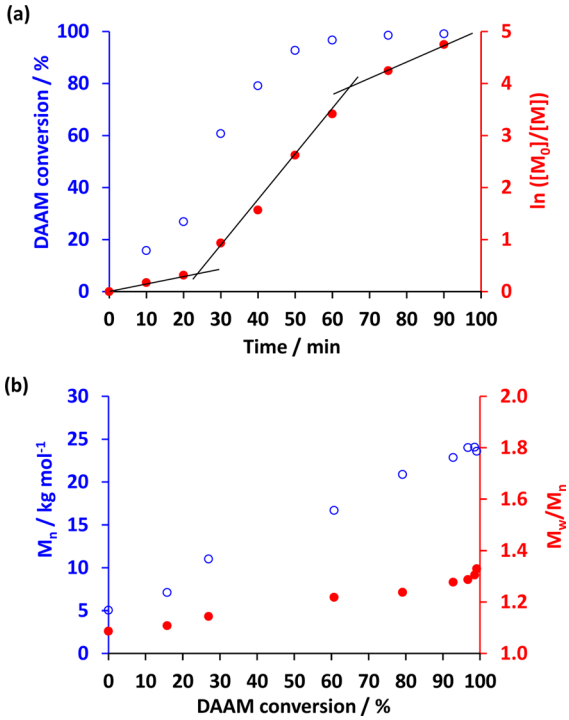

Figure 3. (a) Monomer conversion vs time curve and corresponding $\ln[M_0]/[M]$ plot and (b) evolution of number-average molecular weight (M_n) and dispersity (M_w/M_n) with conversion for the RAFT aqueous dispersion polymerization of DAAM at 70 °C and pH 2.5 using a DDMAT-$PDMAC_{58}$ macro-CTA targeting DDMAT–$PDMAC_{58}$–$PDAAM_{120}$. Conditions: 20% w/w solids and a macro-CTA/AIBN molar ratio of 10.

labeled "I" in Figure 2. The semilogarithmic plot (Figure 3a) indicated more than a 5-fold increase in the rate of polymerization after approximately 25 min, which coincided with the reaction solution becoming distinctly turbid. This indicates the onset of micellar nucleation, with the immediate formation of monomer-swollen particles resulting in a relatively high local DAAM concentration.[27,75] A linear evolution of M_n with DAAM conversion was observed (see Figure 3b), which is consistent with a controlled radical polymerization. However, there was also a modest increase in the copolymer dispersity with conversion, resulting in a final M_w/M_n of 1.33.

Following this kinetic study, a series of $PDMAC_x$–$PDAAM_y$ diblock copolymers were prepared by systematically varying the target PDAAM DP (y), for each of the five $PDMAC_x$ macro-CTAs (where x = 40, 46, 58, 68, or 77). Monomer conversions exceeding 98% were achieved for all such PISA syntheses within 4 h at 70 °C (Table S1). A series of representative GPC chromatograms obtained for $PDMAC_{77}$–$PDAAM_y$ are provided in Figure S2.

PDMAC–PDAAM Diblock Copolymer Characterization. The resulting PDMAC–PDAAM diblock copolymer nano-objects were characterized using transmission electron microscopy (TEM). The assigned morphologies were used to construct a phase diagram at a fixed copolymer concentration of 20% w/w solids. This is shown in Figure 4, along with

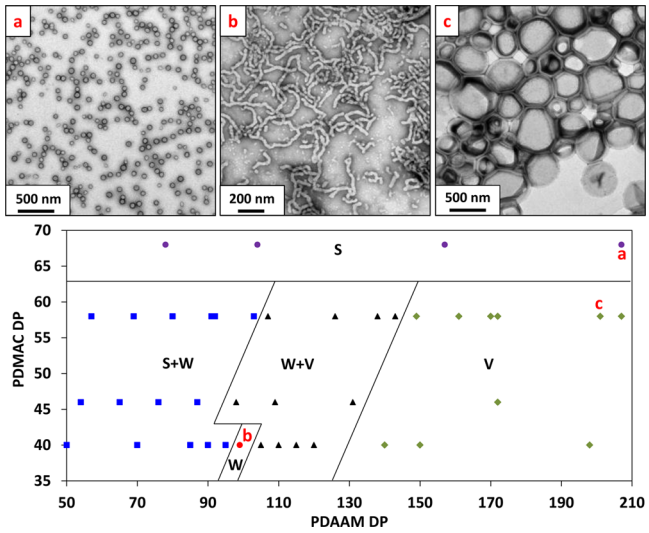

Figure 4. Representative transmission electron microscopy images showing pure sphere, worm, and vesicle morphologies obtained for 0.1% w/w aqueous dispersions of $PDMAC_x$–$PDAAM_y$ diblock copolymer nano-objects at pH 2.5: (a) $PDMAC_{68}$–$PDAAM_{207}$; (b) $PDMAC_{40}$–$PDAAM_{99}$; (c) $PDMAC_{58}$–$PDAAM_{201}$. Phase diagram constructed for a series of $PDMAC_x$–$PDAAM_y$ diblock copolymer nano-objects. S = spheres, S + W = mixed spheres and worms, W = worms, W + V = mixed worms and vesicles and V = vesicles.

representative images of the pure spheres, worms, and vesicles. Only a spherical morphology could be accessed when using a relatively long PDMAC stabilizer block (DP ≥ 68) because such formulations favor elastic collisions between nascent spheres rather than the stochastic 1D sphere–sphere fusion events that lead to the formation of worms. Hence spheres represent a kinetically trapped phase when targeting highly asymmetric diblock compositions.[33] For example, increasing the PDAAM DP from 78 to 620 when using a $PDMAC_{68}$ macro-CTA only resulted in a monotonic increase in mean sphere diameter from 40 to 150 nm, as determined by DLS analysis. In contrast, worms and vesicles could be accessed when using shorter PDMAC macro-CTAs (DP ≤ 58). For example, targeting $PDMAC_x$–$PDAAM_y$ gave pure vesicles when x = 40, 46, and 58 and $y \geq 150$. The phase space for pure

DOI: 10.1021/acs.macromol.6b02643
Macromolecules 2017, 50, 1482–1493

worms was extremely narrow and was bounded by sphere/worm and worm/vesicle mixed phases. Similar observations have been reported by Blanazs and co-workers for an all-methacrylic RAFT aqueous dispersion polymerization formulation.[33] Indeed, pure worms were only attained for $PDMAC_{40}$–$PDAAM_{99}$. This composition resulted in a free-standing gel, most likely as a result of multiple inter-worm contacts.[78] Nevertheless, the phase diagram shown in Figure 4 enables the elusive pure worm phase to be reproducibly targeted.

Lovett et al. reported that poly(glycerol monomethacrylate)–poly(2-hydroxypropyl methacrylate) (PGMA–PHPMA) diblock copolymer nano-objects prepared by RAFT aqueous dispersion polymerization using a carboxylic acid-functionalized CTA exhibit pH-responsive behavior.[63,66] More specifically, worm-to-sphere and vesicle-to-worm transitions were observed on increasing the solution pH from pH 3.5 to pH 6. Such order–order transitions were attributed to ionization of the carboxylic acid end groups on the PGMA chains, which increases the effective volume fraction of this hydrophilic stabilizer block. In the present study, the PDMAC stabilizer blocks also contain a terminal carboxylic acid group, so similar pH-responsive behavior was anticipated. To examine this hypothesis, DLS and aqueous electrophoresis measurements were recorded for a series of 0.1% w/w PDMAC–PDAAM aqueous dispersions as a function of solution pH (see Figure S3). In each case, the zeta potential became more negative at higher pH as a result of deprotonation of the carboxylic acid end-groups on the PDMAC chains originating from the DDMAT RAFT agent. However, the sphere-equivalent particle diameter remained essentially unchanged over the entire pH range studied for PDMA–PDAAM nano-objects synthesized using a relatively long PDMAC macro-CTA (DP $\geq$ 58) or containing a PDAAM block with a mean DP of at least 140 (see Figure S3a–d). Clearly, end-group ionization is insufficient to induce an order–order transition for such copolymers. In contrast, $PDMAC_{40}$–$PDAAM_{99}$ worms proved to be weakly pH-responsive: their sphere-equivalent particle diameter was reduced from 403 nm at pH 2.6 to 208 nm at pH 9.6 (see Figure S3e). TEM studies indicated that this is the result of a transition from pure worms to a mixed phase comprising relatively short worms and spheres (Figure S3f).

There are numerous literature examples of thermoresponsive diblock copolymer nano-objects prepared by RAFT aqueous dispersion polymerization. Such behavior has been reported for relatively weakly hydrophobic core-forming blocks such as PHPMA, PNIPAM, and PMEA.[18,29,63−65] Given that the DAAM monomer is fully miscible with water, the corresponding PDAAM block might be expected to be weakly hydrophobic and partially hydrated, as previously reported for PHPMA.[64] For $PDMAC_{58}$–$PDAAM_y$ nano-objects, no change in either solution viscosity or turbidity was observed when cooling 20% w/w aqueous dispersions of spheres, worms, or vesicles to below 5 °C or on heating up to 50 °C. DLS studies confirmed that no discernible change in hydrodynamic diameter occurred on either heating or cooling a 0.1% w/w aqueous dispersion of $PDMAC_{58}$–$PDAAM_{170}$ vesicles at pH 2.5 (Figure S4a). [One reviewer of this manuscript has suggested that hydrogen bonding between the amide repeat units might be responsible for this unexpected lack of thermosensitivity.] In contrast, a modest reduction in the sphere-equivalent particle diameter from approximately 360 nm to around 300 nm was observed for a 0.1% w/w aqueous dispersion of $PDMAC_{40}$–$PDAAM_{99}$ worms on heating from 20 to 50 °C (see Figure S4b). TEM studies indicate that this is the result of a morphological transition from worms to a mixture of short worms and vesicles (see Figure S4c). Similar thermoresponsive behavior has been previously observed for aqueous dispersions of diblock copolymer nano-objects.[63,64,66] This transition is believed to be related to the relatively narrow phase space occupied by these pure worms (see Figure 4).

In summary, $PDMAC_x$–$PDAAM_y$ diblock copolymer nano-objects with $x \geq 58$ or $y \geq 140$ prepared herein proved to be neither pH-responsive on raising the solution pH to pH 10 nor thermoresponsive on lowering the solution temperature to 5 °C or heating to 50 °C. In contrast, $PDMAC_{40}$–$PDAAM_{99}$ worms proved to be weakly responsive with respect to changes to either solution pH or temperature. However, it is perhaps noteworthy that unlike the observations made by Lovett and co-workers,[66] no *additional* change in copolymer morphology was observed when subjecting these $PDMAC_{40}$–$PDAAM_{99}$ worms to a *dual* stimulus-response (i.e., switching the solution pH to pH 9 while simultaneously cooling to 5 °C, or heating to 50 °C).

Covalent Stabilization of PDMAC–PDAAM Diblock Copolymer Nano-Objects. All PISA syntheses were conducted at an initial solution pH of 2.5. However, for the 20% w/w formulations reported herein, the solution pH had risen in each case to approximately 4 after DAAM polymerization. Fortuitously, this is the optimum pH for subsequent cross-linking using ADH, as reported by Kessel et al.[59] This reagent's hydrazide groups can react with the pendent ketone groups on the PDAAM chains via nucleophilic substitution to form hydrazone linkages (Scheme 2). If the two hyrazide groups on ADH react with different PDAAM chains, then this should result in covalent stabilization of these nano-objects. All such cross-linking reactions were conducted at 25 °C using various ADH/DAAM molar ratios.

Spectroscopic evidence for the proposed cross-linking reaction was obtained from FT-IR studies. First, a model reaction was conducted whereby a stirred 20% w/w aqueous solution of DAAM monomer was reacted with ADH using an ADH/DAAM molar ratio of 0.50 at 25 °C. This reaction mixture gradually became turbid, and after 6 h the crude product was isolated by freeze-drying overnight. FT-IR spectra recorded for ADH alone, the DAAM monomer, and the freeze-dried crude product are shown in Figure 5.

The DAAM monomer spectrum has a strong ketone band at 1716 cm^{-1}. This characteristic feature is absent in the product, indicating loss of the ketone moiety. Complete attenuation of this ketone band confirms efficient reaction of the ADH with DAAM monomer within 6 h at 25 °C.

Following this successful model reaction, a FT-IR study of the addition of ADH to an aqueous dispersion of $PDMAC_{58}$–$PDAAM_{230}$ vesicles was undertaken. Figure 6 shows the FT-IR spectra recorded for (a) ADH alone, (b) the original linear freeze-dried $PDMAC_{58}$–$PDAAM_{230}$ vesicles, and (c) a freeze-dried 20% w/w $PDMAC_{58}$–$PDAAM_{230}$ vesicle dispersion after ADH cross-linking using an ADH/DAAM molar ratio of 0.50 for 6 h at 25 °C.

The pendent ketone groups in the PDAAM chains exhibit a characteristic band at 1707 cm^{-1}, which is close to that observed for DAAM monomer (see above). After cross-linking with ADH for 6 h at 25 °C, this spectral feature became substantially attenuated relative to the other IR bands. However, the remaining shoulder observed for the cross-linked

DOI: 10.1021/acs.macromol.6b02643
Macromolecules 2017, 50, 1482–1493

Scheme 2. Reaction Scheme Illustrating the Acid-Catalyzed Nucleophilic Attack of PDAAM Pendent Ketone Groups by Adipic Acid Dihydrazide (ADH)[a]

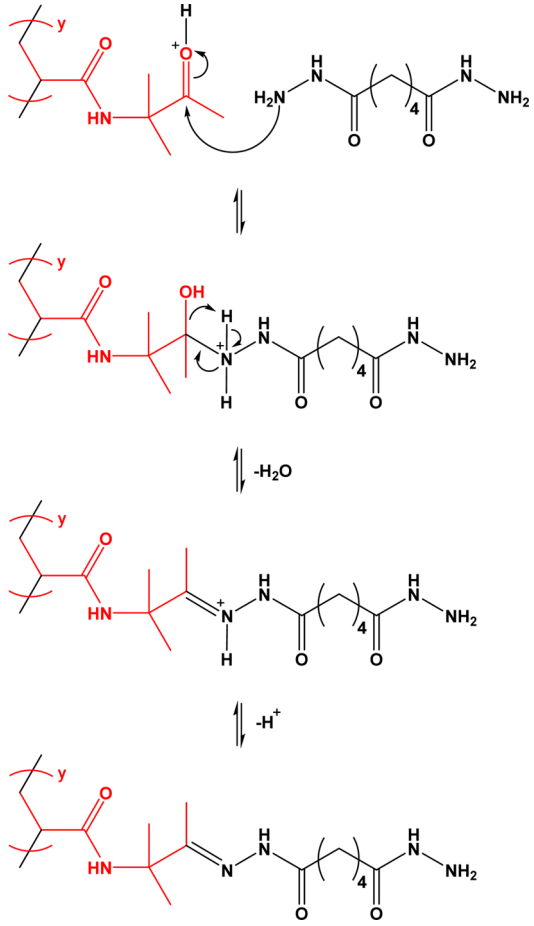

[a]If the pendent hydrazine group then reacts with a ketone group on a second PDAAM chain, this leads to cross-linking.

PDMAC−PDAAM vesicles suggests that cross-linking remained incomplete after 6 h. It is also worth emphasizing that reaction of the ADH with the pendent ketone groups on the PDAAM chains does not necessarily guarantee that an intermolecular cross-link is obtained. It is likely that at least some of the ADH is consumed in the formation of intramolecular cycles via reaction with two ketones located on the same PDAAM chain.[77−79] Moreover, it is also possible that the ADH might only react once, with its second hydrazide group being simply unable to react with another ketone group because of steric congestion. This latter problem is more likely to occur at higher degrees of cross-linking as the PDAAM cores become more solidlike.

FT-IR spectra recorded when cross-linking $PDMAC_{58}$−$PDAAM_{230}$ vesicles using ADH/DAAM molar ratios of 1.00, 0.50, 0.25, or 0.10 indicated that greater attenuation of the ketone band occurred at higher ADH concentrations (see Figure S5). The effect of varying the ADH concentration on the extent of cross-linking (and hence degree of covalent stabilization of the nano-objects) was studied using DLS. Accordingly, ADH was added to a 20% w/w aqueous dispersion of $PDMAC_{58}$−$PDAAM_{230}$ vesicles at ADH/DAAM molar ratios of 0.010, 0.025, 0.050, 0.075, 0.100, 0.150, or 0.200 and allowed to react at 25 °C with continuous stirring for 24 h.

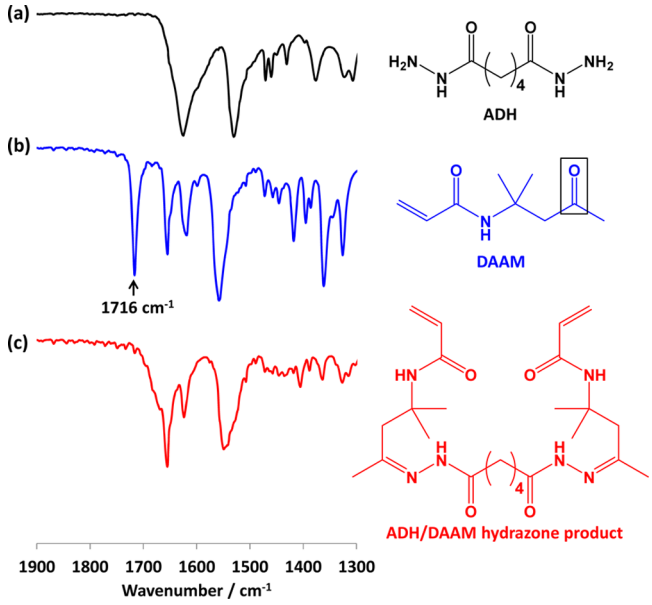

Figure 5. FT-IR spectra recorded for (a) adipic acid dihydrazide (ADH) cross-linker, (b) DAAM monomer, and (c) the freeze-dried product obtained from the reaction of ADH with DAAM at 25 °C for 6 h using an ADH/DAAM molar ratio of 0.50. Conditions: 20% w/w solution, pH 2.5.

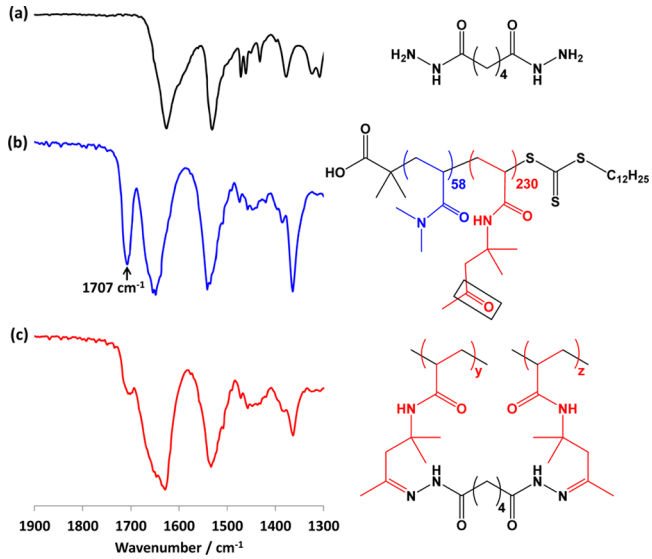

Figure 6. FT-IR spectra recorded for (a) the adipic acid dihydrazide (ADH) cross-linker alone, (b) a freeze-dried 20% w/w aqueous dispersion of $PDMAC_{58}$−$PDAAM_{230}$ vesicles, and (c) the freeze-dried product of the reaction of a 20% w/w aqueous dispersion of $PDMAC_{58}$−$PDAAM_{230}$ vesicles with ADH. Conditions: ADH/DAAM molar ratio = 0.50, 6 h, 25 °C, pH 4.

Aliquots taken at various time intervals were diluted to 0.1% w/v in methanol, which is a good solvent for both PDMAC and PDAAM. Thus, if no cross-linking had occurred, then molecular dissolution would be expected in this solvent. All these dilute methanolic dispersions were analyzed by DLS to establish the minimum time required for sufficient covalent stabilization to preserve the original nano-objects. As ADH cross-linking progressed, the vesicles became gradually more resistant to methanol dissolution. For each ADH concentration, the scattered light intensity (or derived count rate) and the

DOI: 10.1021/acs.macromol.6b02643
Macromolecules 2017, 50, 1482−1493

sphere-equivalent particle diameter were monitored as a function of time (see Figure 7). The former parameter

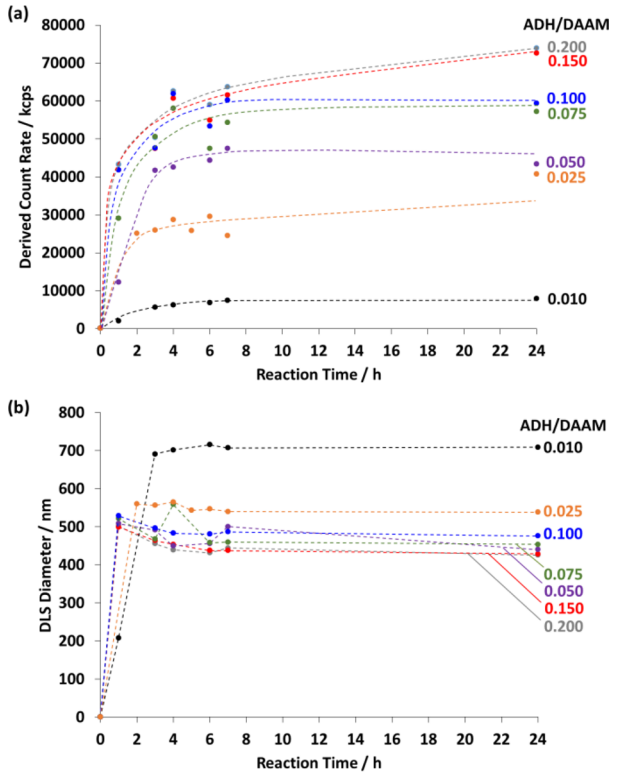

Figure 7. Time dependence for (a) scattered light intensity count rate and (b) DLS diameter when cross-linking a 20% w/w aqueous dispersion of $PDMAC_{58}$–$PDAAM_{230}$ vesicles at pH 4 using ADH at ADH/DAAM molar ratios of 0.200, 0.150, 0.100, 0.075, 0.050, 0.025, or 0.010 at 25 °C. Aliquots were extracted from the reaction solution at regular time intervals prior to quenching via dilution to 0.1% w/v solids using methanol (which is a good solvent for both blocks and hence causes molecular dissolution if the degree of vesicle cross-linking is insufficient to ensure covalent stabilization).

increased up to approximately 6 h, after which plateau values were observed (Figure 7a). This suggests that the cross-linking was close to completion on this time scale. Moreover, maximum covalent stabilization was achieved for ADH/DAAM molar ratios ≥0.075.

The DLS diameter for a dilute aqueous dispersion of $PDMAC_{58}$–$PDAAM_{230}$ vesicles (0.1% w/w at pH 2.5) prior to cross-linking was 402 nm. Figure 7b indicates that larger particle diameters were observed for all ADH concentrations as a result of swelling of the cross-linked vesicles when diluted in methanol. Substantial swelling was observed for the lightly cross-linked vesicles in the presence of methanol. In contrast, much less swelling occurred for ADH/DAAM molar ratios ≥0.050 because more extensive cross-linking was obtained under these conditions. TEM images of the linear $PDMAC_{58}$–$PDAAM_{230}$ vesicles and a series of vesicles cross-linked using various ADH/DAAM molar ratios are shown in Figure S6. Retention of the original vesicle morphology after dilution in methanol confirms covalent stabilization.

Cross-linking was also conducted on aqueous dispersions of $PDMAC_{68}$–$PDAAM_{207}$ spheres and $PDMAC_{40}$–$PDAAM_{99}$ worms (ADH/DAAM molar ratio = 0.100; 6 h at 25 °C). In both cases, the original copolymer morphology was retained on exposure to methanol as determined by TEM analysis (Figure 8). Swelling of the cross-linked $PDMAC_{68}$–$PDAAM_{207}$ spheres in methanol resulted in a larger DLS diameter of 77 nm

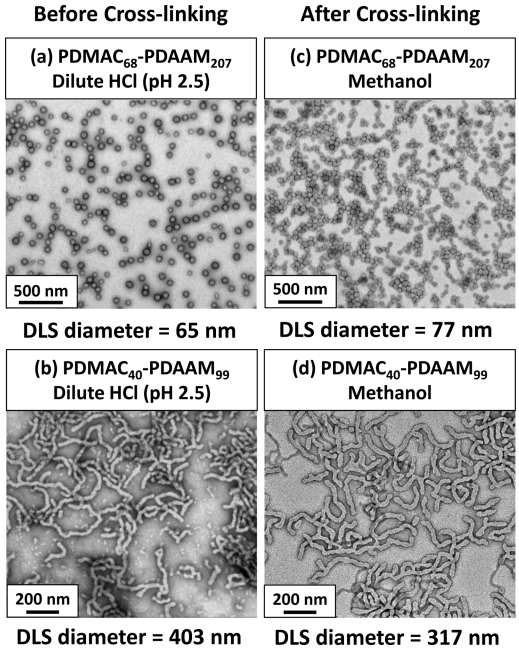

Figure 8. TEM images and DLS measurements recorded for 0.1% *aqueous* dispersions of (a) linear $PDMAC_{68}$–$PDAAM_{207}$ spheres and (b) linear $PDMAC_{40}$–$PDAAM_{99}$ worms at pH 2.5; 0.1% *methanolic* dispersions of (c) cross-linked $PDMAC_{68}$–$PDAAM_{207}$ spheres and (d) cross-linked $PDMAC_{40}$–$PDAAM_{99}$ worms after reacting with ADH at an ADH/DAAM molar ratio of 0.10 for 6 h at 25 °C.

(compared to 65 nm measured at pH 2.5 prior to cross-linking). Conversely, the sphere-equivalent diameter obtained for the cross-linked $PDMAC_{40}$-$PDAAM_{99}$ worms was *lower* than that determined prior to cross-linking (317 nm vs 403 nm). Given that the TEM images shown in Figure 8 confirm retention of the worm morphology, one possible explanation for these DLS observations is that insufficient worm cross-linking may result in partial worm fragmentation on exposure to methanol.

Rheological Studies. The storage modulus, G', of a 20% w/w $PDMAC_{40}$–$PDAAM_{99}$ worm gel was determined by oscillatory rheology before and after ADH cross-linking for 6 h at 25 °C using a ADH/DAAM molar ratio of 0.10. At a fixed angular frequency of 1.0 rad s^{-1} and a constant strain of 1.0%, G' increased from 2 370 Pa to 10 330 Pa at 25 °C (see Figure 9). Similar enhancements in gel strength on cross-linking were also reported by both Lovett et al.[80] and Bates and co-workers.[81] This has been attributed to worm stiffening, which leads to an increase in the worm mean persistence length.

CONCLUSIONS

In summary, a series of well-defined hydrophilic PDMAC macro-CTAs (mean DPs = 40, 46, 58, 68, or 77) were prepared using DDMAT and subsequently chain-extended with DAAM using a RAFT aqueous dispersion polymerization formulation. The resulting amphiphilic diblock copolymers formed a range of nano-objects via polymerization-induced self-assembly. A phase diagram was constructed for various diblock copolymer compositions at 20% w/w solids. Pure spheres, worms, and vesicles were identified by TEM studies. The worm phase space

DOI: 10.1021/acs.macromol.6b02643
Macromolecules 2017, 50, 1482–1493

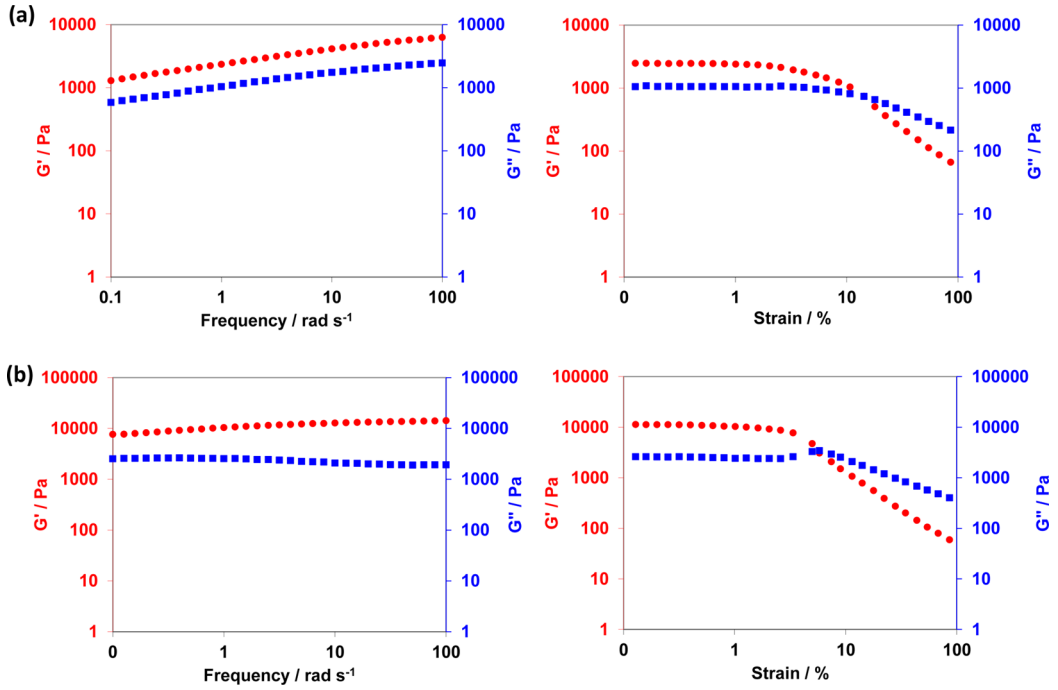

Figure 9. Variation of gel moduli (G', red circles; G'', blue squares) with frequency at an applied strain of 1.0% and variation of gel moduli (G', red circles; G'', blue squares) with strain at an applied frequency of 1 rad s^{-1} for (a) linear $PDMAC_{40}$–$PDAAM_{99}$ diblock copolymer prepared at 20% w/w solids in water at pH 2.5 and (b) cross-linked $PDMAC_{40}$–$PDAAM_{99}$ diblock copolymer prepared at 20% w/w solids in water at pH 2.5 with subsequent cross-linking at 25 °C for 6 h (ADH/DAAM molar ratio = 0.10).

was extremely narrow, which no doubt explains why this copolymer morphology had not been previously identified for this particular PISA formulation.[51]

Remarkably, most of these PDMAC–PDAAM nano-objects proved to be insensitive to changes in both solution temperature and pH. This behavior is atypical compared to other RAFT aqueous dispersion polymerization formulations based on HPMA, NIPAM, or MEA,[18,29,63,64] where such water-miscible monomers normally produce rather weakly hydrophobic structure-directing blocks with significant degrees of plasticization.[23] However, the $PDMAC_{40}$–$PDAAM_{99}$ worms did prove to be both weakly pH-responsive and thermosensitive: this is attributed to the extremely narrow phase space occupied by this copolymer morphology, and perhaps also the relatively low mean DP for each block.

Concentrated aqueous dispersions of covalently stabilized diblock copolymer nano-objects could be prepared at ambient temperature using adipic acid dihydrazide (ADH), which reacts selectively with the pendent ketone groups on the hydrophobic PDAAM chains to form hydrazone moieties. FT-IR studies provided direct spectroscopic evidence for this cross-linking chemistry, while DLS measurements performed in methanol (a good solvent for the PDMAC and PDAAM blocks) confirmed that covalent stabilization could be achieved within 6 h at 25 °C using ADH/DAAM molar ratios as low as 0.075. Finally, rheological studies indicated a 4-fold increase in worm gel strength when using a DAAM/ADH molar ratio of 0.100, presumably because cross-linking leads to an increase in the worm persistence length.

■ ASSOCIATED CONTENT

Supporting Information

The Supporting Information is available free of charge on the ACS Publications website at DOI: 10.1021/acs.macromol.6b02643.

UV spectra and Beer–Lambert plot for DDMAT CTA; additional DMF GPC data; summary table of characterization data for all diblock copolymers; additional DLS and zeta potential data as a function of pH, temperature; additional TEM images and FT-IR spectra (PDF)

■ AUTHOR INFORMATION

Corresponding Author

*E-mail: S.P.Armes@sheffield.ac.uk (S.P.A.).

ORCID

Steven P. Armes: 0000-0002-8289-6351

Notes

The authors declare no competing financial interest.

■ ACKNOWLEDGMENTS

We thank EPSRC and BASF (Ludwigshafen, Germany) for a CDT PhD studentship for S.J.B. S.P.A. also acknowledges an ERC Advanced Investigator grant (PISA 320372).

■ REFERENCES

(1) Blanazs, A.; Armes, S. P.; Ryan, A. J. Self-Assembled Block Copolymer Aggregates: From Micelles to Vesicles and Their Biological Applications. *Macromol. Rapid Commun.* **2009**, *30*, 267–277.

(2) Choucair, A.; Eisenberg, A. Control of Amphiphilic Block Copolymer Morphologies Using Solution Conditions. *Eur. Phys. J. E: Soft Matter Biol. Phys.* **2003**, *10*, 37–44.

(3) Discher, D. E.; Eisenberg, A. Polymer Vesicles. *Science* **2002**, *297*, 967–973.

DOI: 10.1021/acs.macromol.6b02643
Macromolecules 2017, 50, 1482–1493

(4) Jain, S.; Bates, F. S. On the Origins of Morphological Complexity in Block Copolymer Surfactants. *Science* **2003**, *300*, 460−464.
(5) Förster, S.; Zisenis, M.; Wenz, E.; Antonietti, M. Micellization of Strongly Segregated Block Copolymers. *J. Chem. Phys.* **1996**, *104*, 9956−9970.
(6) Bang, J.; Jain, S.; Li, Z.; Lodge, T. P.; et al. Sphere, Cylinder, and Vesicle Nanoaggregates in Poly(styrene-B-Isoprene) Diblock Copolymer Solutions. *Macromolecules* **2006**, *39*, 1199−1208.
(7) Zhang, L.; Eisenberg, A. Multiple Morphologies of "Crew-Cut " Aggregates of Polystyrene-B-Poly(acrylic Acid) Block Copolymers. *Science* **1995**, *268*, 1728−1731.
(8) Yu, K.; Eisenberg, A. Multiple Morphologies in Aqueous Solutions of Aggregates of Polystyrene-Block-Poly(ethylene Oxide) Diblock Copolymers. *Macromolecules* **1996**, *29*, 6359−6361.
(9) Discher, B. M.; Won, Y.; Ege, D. S.; Lee, J. C.-M.; Bates, F. S.; Discher, D. E.; Hammer, D. A. Polymersomes: Tough Vesicles Made from Diblock Copolymers. *Science* **1999**, *284*, 1143−1146.
(10) Hayward, R. C.; Pochan, D. J. Tailored Assemblies of Block Copolymers in Solution: It Is All about the Process. *Macromolecules* **2010**, *43*, 3577−3584.
(11) Gao, Z.; Varshney, S. K.; Wong, S.; Eisenberg, A. Block Copolymer "Crew-Cut" Micelles in Water. *Macromolecules* **1994**, *27*, 7923−7927.
(12) Zhang, L.; Eisenberg, A. Multiple Morphologies and Characteristics of "Crew-Cut" Aggregates of Polystyrene-B-Poly(acrylic Acid) Diblock Copolymers in Aqueous Solutions. *J. Am. Chem. Soc.* **1996**, *118*, 3168−3181.
(13) Cunningham, V. J.; Alswieleh, A. M.; Thompson, K. L.; Williams, M.; Leggett, G. J.; Armes, S. P.; Musa, O. M. Poly(glycerol Monomethacrylate)-Poly(benzyl Methacrylate) Diblock Copolymer Nanoparticles via RAFT Emulsion Polymerization: Synthesis, Characterization, and Interfacial Activity. *Macromolecules* **2014**, *47*, 5613−5623.
(14) Li, Y.; Armes, S. P. RAFT Synthesis of Sterically Stabilized Methacrylic Nanolatexes and Vesicles by Aqueous Dispersion Polymerization. *Angew. Chem., Int. Ed.* **2010**, *49*, 4042−4046.
(15) Liu, G.; Qiu, Q.; Shen, W.; An, Z. Aqueous Dispersion Polymerization of 2-Methoxyethyl Acrylate for the Synthesis of Biocompatible Nanoparticles Using a Hydrophilic RAFT Polymer and a Redox Initiator. *Macromolecules* **2011**, *44*, 5237−5245.
(16) Boissé, S.; Rieger, J.; Belal, K.; Di-Cicco, A.; Beaunier, P.; Li, M.-H.; Charleux, B. Amphiphilic Block Copolymer Nano-Fibers via RAFT-Mediated Polymerization in Aqueous Dispersed System. *Chem. Commun.* **2010**, *46*, 1950−1952.
(17) Ferguson, C. J.; Hughes, R. J.; Nguyen, D.; Pham, B. T. T.; Gilbert, R. G.; Serelis, A. K.; Such, C. H.; Hawkett, B. S. Ab Initio Emulsion Polymerization by RAFT-Controlled Self-Assembly. *Macromolecules* **2005**, *38*, 2191−2204.
(18) An, Z.; Shi, Q.; Tang, W.; Tsung, C. K.; Hawker, C. J.; Stucky, G. D. Facile RAFT Precipitation Polymerization for the Microwave-Assisted Synthesis of Well-Defined, Double Hydrophilic Block Copolymers and Nanostructured Hydrogels. *J. Am. Chem. Soc.* **2007**, *129*, 14493−14499.
(19) Binauld, S.; Delafresnaye, L.; Charleux, B.; D'agosto, F.; Lansalot, M. Emulsion Polymerization of Vinyl Acetate in the Presence of Different Hydrophilic Polymers Obtained by RAFT/MADIX. *Macromolecules* **2014**, *47*, 3461−3472.
(20) Sugihara, S.; Ma'Radzi, A. H.; Ida, S.; Irie, S.; Kikukawa, T.; Maeda, Y. In Situ Nano-Objects via RAFT Aqueous Dispersion Polymerization of 2-Methoxyethyl Acrylate Using Poly(ethylene Oxide) Macromolecular Chain Transfer Agent as Steric Stabilizer. *Polymer* **2015**, *76*, 17−24.
(21) Canning, S. L.; Smith, G. N.; Armes, S. P. A Critical Appraisal of RAFT-Mediated Polymerization-Induced Self-Assembly. *Macromolecules* **2016**, *49*, 1985−2001.
(22) Derry, M. J.; Fielding, L. A.; Armes, S. P. Polymerization-Induced Self-Assembly of Block Copolymer Nanoparticles via RAFT Non-Aqueous Dispersion Polymerization. *Prog. Polym. Sci.* **2016**, *52*, 1−18.
(23) Warren, N. J.; Armes, S. P. Polymerization-Induced Self-Assembly of Block Copolymer Nano-Objects via RAFT Aqueous Dispersion Polymerization. *J. Am. Chem. Soc.* **2014**, *136*, 10174−10185.
(24) Canton, I.; Warren, N. J.; Chahal, A.; Amps, K.; Wood, A.; Weightman, R.; Wang, E.; Moore, H.; Armes, S. P. Mucin-Inspired Thermoresponsive Synthetic Hydrogels Induce Stasis in Human Pluripotent Stem Cells and Human Embryos. *ACS Cent. Sci.* **2016**, *2*, 65−74.
(25) Mitchell, D. E.; Lovett, J. R.; Armes, S. P.; Gibson, M. I. Combining Biomimetic Block Copolymer Worms with an Ice-Inhibiting Polymer for the Solvent-Free Cryopreservation of Red Blood Cells. *Angew. Chem., Int. Ed.* **2016**, *55*, 2801−2804.
(26) Ladmiral, V.; Semsarilar, M.; Canton, I.; Armes, S. P. Polymerization-Induced Self-Assembly of Galactose-Functionalized Biocompatible Diblock Copolymers for Intracellular Delivery. *J. Am. Chem. Soc.* **2013**, *135*, 13574−13581.
(27) Blanazs, A.; Madsen, J.; Battaglia, G.; Ryan, A. J.; Armes, S. P. Mechanistic Insights for Block Copolymer Morphologies: How Do Worms Form Vesicles? *J. Am. Chem. Soc.* **2011**, *133*, 16581−16587.
(28) Sugihara, S.; Blanazs, A.; Armes, S. P.; Ryan, A. J.; Lewis, A. L. Aqueous Dispersion Polymerization: A New Paradigm for In Situ Block Copolymer Self-Assembly in Concentrated Solution. *J. Am. Chem. Soc.* **2011**, *133*, 15707−15713.
(29) Liu, G.; Qiu, Q.; An, Z. Development of Thermosensitive Copolymers of Poly(2-Methoxyethyl Acrylate-Co-Poly(ethylene Glycol) Methyl Ether Acrylate) and Their Nanogels Synthesized by RAFT Dispersion Polymerization in Water. *Polym. Chem.* **2012**, *3*, 504−513.
(30) Shen, W.; Chang, Y.; Liu, G.; Wang, H.; Cao, A.; An, Z. Biocompatible, Antifouling, and Thermosensitive Core−Shell Nanogels Synthesized by RAFT Aqueous Dispersion Polymerization. *Macromolecules* **2011**, *44*, 2524−2530.
(31) Rieger, J.; Grazon, C.; Charleux, B.; Alaimo, D.; Jérôme, C. Pegylated Thermally Responsive Block Copolymer Micelles and Nanogels via In Situ RAFT Aqueous Dispersion Polymerization. *J. Polym. Sci., Part A: Polym. Chem.* **2009**, *47*, 2373−2390.
(32) Grazon, C.; Rieger, J.; Sanson, N.; Charleux, B. Study of Poly(N,N-Diethylacrylamide) Nanogel Formation by Aqueous Dispersion Polymerization of N,N-Diethylacrylamide in the Presence of Poly(ethylene Oxide)-B-Poly(N,N-Dimethylacrylamide) Amphiphilic Macromolecular RAFT Agents. *Soft Matter* **2011**, *7*, 3482−3490.
(33) Blanazs, A.; Ryan, A. J.; Armes, S. P. Predictive Phase Diagrams for RAFT Aqueous Dispersion Polymerization: Effect of Block Copolymer Composition, Molecular Weight, and Copolymer Concentration. *Macromolecules* **2012**, *45*, 5099−5107.
(34) Semsarilar, M.; Ladmiral, V.; Blanazs, A.; Armes, S. P. Anionic Polyelectrolyte-Stabilized Nanoparticles via RAFT Aqueous Dispersion Polymerization. *Langmuir* **2012**, *28*, 914−922.
(35) Semsarilar, M.; Ladmiral, V.; Blanazs, A.; Armes, S. P. Cationic Polyelectrolyte-Stabilized Nanoparticles via RAFT Aqueous Dispersion Polymerization. *Langmuir* **2013**, *29*, 7416−7424.
(36) Ladmiral, V.; Charlot, A.; Semsarilar, M.; Armes, S. P. Synthesis and Characterization of Poly(amino Acid Methacrylate)-Stabilized Diblock Copolymer Nano-Objects. *Polym. Chem.* **2015**, *6*, 1805−1816.
(37) Chaduc, I.; Crepet, A.; Boyron, O.; Charleux, B.; D'Agosto, F.; Lansalot, M. Effect of the pH on the RAFT Polymerization of Acrylic Acid in Water. Application to the Synthesis of Poly(acrylic Acid)-Stabilized Polystyrene Particles by RAFT Emulsion Polymerization. *Macromolecules* **2013**, *46*, 6013−6023.
(38) Zhang, X.; Boissé, S.; Zhang, W.; Beaunier, P.; D'Agosto, F.; Rieger, J.; Charleux, B. Well-Defined Amphiphilic Block Copolymers and Nano-Objects Formed in Situ via RAFT-Mediated Aqueous Emulsion Polymerization. *Macromolecules* **2011**, *44*, 4149−4158.
(39) Zhang, W.; D'Agosto, F.; Dugas, P. Y.; Rieger, J.; Charleux, B. RAFT-Mediated One-Pot Aqueous Emulsion Polymerization of Methyl Methacrylate in Presence of Poly(methacrylic Acid-Co-Poly(ethylene Oxide) Methacrylate) Trithiocarbonate Macromolecular Chain Transfer Agent. *Polymer* **2013**, *54*, 2011−2019.

DOI: 10.1021/acs.macromol.6b02643
Macromolecules 2017, 50, 1482−1493

(40) Zhang, W.; D'Agosto, F.; Boyron, O.; Rieger, J.; Charleux, B. One-Pot Synthesis of Poly(methacrylic Acid-Co-Poly(ethylene Oxide) Methyl Ether Methacrylate)-B-Polystyrene Amphiphilic Block Copolymers and Their Self-Assemblies in Water via RAFT-Mediated Radical Emulsion Polymerization. A Kinetic Study. *Macromolecules* **2011**, *44*, 7584−7593.
(41) Zhang, W.; D'Agosto, F.; Boyron, O.; Rieger, J.; Charleux, B. Toward a Better Understanding of the Parameters That Lead to the Formation of Nonspherical Polystyrene Particles via RAFT-Mediated One-Pot Aqueous Emulsion Polymerization. *Macromolecules* **2012**, *45*, 4075−4084.
(42) Truong, N. P.; Dussert, M. V.; Whittaker, M. R.; Quinn, J. F.; Davis, T. P. Rapid Synthesis of Ultrahigh Molecular Weight and Low Polydispersity Polystyrene Diblock Copolymers by RAFT-Mediated Emulsion Polymerization. *Polym. Chem.* **2015**, *6*, 3865−3874.
(43) Rieger, J.; Zhang, W.; Stoffelbach, F.; Charleux, B. Surfactant-Free RAFT Emulsion Polymerization Using Poly(N,N-Dimethylacrylamide) Trithiocarbonate Macromolecular Chain Transfer Agents. *Macromolecules* **2010**, *43*, 6302−6310.
(44) Ning, Y.; Fielding, L. A.; Ratcliffe, L. P. D.; Wang, Y.-W.; Meldrum, F. C.; Armes, S. P. Occlusion of Sulfate-Based Diblock Copolymer Nanoparticles within Calcite: Effect of Varying the Surface Density of Anionic Stabilizer Chains. *J. Am. Chem. Soc.* **2016**, *138*, 11734−11742.
(45) Rieger, J.; Stoffelbach, F.; Bui, C.; Alaimo, D.; Jérôme, C.; Charleux, B. Amphiphilic Poly(ethylene Oxide) Macromolecular RAFT Agent as a Stabilizer and Control Agent in Ab Initio Batch Emulsion Polymerization. *Macromolecules* **2008**, *41*, 4065−4068.
(46) Chaduc, I.; Girod, M.; Antoine, R.; Charleux, B.; D'Agosto, F.; Lansalot, M. Batch Emulsion Polymerization Mediated by Poly(methacrylic Acid) MacroRAFT Agents: One-Pot Synthesis of Self-Stabilized Particles. *Macromolecules* **2012**, *45*, 5881−5893.
(47) Boissé, S.; Rieger, J.; Pembouong, G.; Beaunier, P.; Charleux, B. Influence of the Stirring Speed and $CaCl_2$ Concentration on the Nano-Object Morphologies Obtained via RAFT-Mediated Aqueous Emulsion Polymerization in the Presence of a Water-Soluble macroRAFT Agent. *J. Polym. Sci., Part A: Polym. Chem.* **2011**, *49*, 3346−3354.
(48) Lesage de la Haye, J.; Zhang, X.; Chaduc, I.; Brunel, F.; Lansalot, M.; D'Agosto, F. The Effect of Hydrophile Topology in RAFT-Mediated Polymerization-Induced Self-Assembly. *Angew. Chem., Int. Ed.* **2016**, *55*, 3739−3743.
(49) Chambon, P.; Blanazs, A.; Battaglia, G.; Armes, S. P. Facile Synthesis of Methacrylic ABC Triblock Copolymer Vesicles by RAFT Aqueous Dispersion Polymerization. *Macromolecules* **2012**, *45*, 5081−5090.
(50) Ratcliffe, L. P. D.; Ryan, A. J.; Armes, S. P. From a Water-Immiscible Monomer to Block Copolymer Nano-Objects via a One-Pot RAFT Aqueous Dispersion Polymerization Formulation. *Macromolecules* **2013**, *46*, 769−777.
(51) Zhou, W.; Qu, Q.; Xu, Y.; An, Z. Aqueous Polymerization-Induced Self-Assembly for the Synthesis of Ketone-Functionalized Nano-Objects with Low Polydispersity. *ACS Macro Lett.* **2015**, *4*, 495−499.
(52) Yu, Q.; Ding, Y.; Cao, H.; Lu, X.; Cai, Y. Use of Polyion Complexation for Polymerization-Induced Self-Assembly in Water under Visible Light Irradiation at 25 °C. *ACS Macro Lett.* **2015**, *4*, 1293−1296.
(53) Jiang, Y.; Xu, N.; Han, J.; Yu, Q.; Guo, L.; Gao, P.; Lu, X.; Cai, Y. The Direct Synthesis of Interface-Decorated Reactive Block Copolymer Nanoparticles via Polymerisation-Induced Self-Assembly. *Polym. Chem.* **2015**, *6*, 4955−4965.
(54) Qu, Q.; Liu, G.; Lv, X.; Zhang, B.; An, Z. In Situ Cross-Linking of Vesicles in Polymerization-Induced Self-Assembly. *ACS Macro Lett.* **2016**, *5*, 316−320.
(55) Gao, P.; Cao, H.; Ding, Y.; Cai, M.; Cui, Z.; Lu, X.; Cai, Y. Synthesis of Hydrogen-Bonded Pore-Switchable Cylindrical Vesicles via Visible-Light-Mediated RAFT Room-Temperature Aqueous Dispersion Polymerization. *ACS Macro Lett.* **2016**, *5*, 1327−1331.
(56) Xu, Y.; Li, Y.; Cao, X.; Chen, Q.; An, Z. Versatile RAFT Dispersion Polymerization in Cononsolvents for the Synthesis of Thermoresponsive Nanogels with Controlled Composition, Functionality and Architecture. *Polym. Chem.* **2014**, *5*, 6244−6255.
(57) Daigle, J.-C.; Arnold, A. A.; Piche, L.; Claverie, J. P. A Functional Polymer with Chemically Switchable Crystallinity. *Polym. Chem.* **2013**, *4*, 449−452.
(58) Ishii, D.; Takahashi, A.; Shimomura, M. Biomimetic Hydrophilic-Hydrophobic Hybrid Polymer-Structured Surfaces with Superhydrophobicity and Strong Water Microdroplet Adhesion. *Chem. Lett.* **2012**, *41*, 1276−1278.
(59) Kessel, N.; Illsley, D. R.; Keddie, J. L. The Diacetone Acrylamide Crosslinking Reaction and Its Influence on the Film Formation of an Acrylic Latex. *J. Coatings Technol. Res.* **2008**, *5*, 285−297.
(60) Mukherjee, S.; Hill, M. R.; Sumerlin, B. S. Self-Healing Hydrogels Containing Reversible Oxime Crosslinks. *Soft Matter* **2015**, *11*, 6152−6161.
(61) Lopez-Oliva, A. P.; Warren, N. J.; Rajkumar, A.; Mykhaylyk, O. O.; Derry, M. J.; Doncom, K. E. B.; Rymaruk, M. J.; Armes, S. P. Polydimethylsiloxane-Based Diblock Copolymer Nano-Objects Prepared in Nonpolar Media via RAFT-Mediated Polymerization-Induced Self-Assembly. *Macromolecules* **2015**, *48*, 3547−3555.
(62) Semsarilar, M.; Penfold, N. J. W.; Jones, E. R.; Armes, S. P. Semi-Crystalline Diblock Copolymer Nano-Objects Prepared via RAFT Alcoholic Dispersion Polymerization of Stearyl Methacrylate. *Polym. Chem.* **2015**, *6*, 1751−1757.
(63) Lovett, J. R.; Warren, N. J.; Armes, S. P.; Smallridge, M. J.; Cracknell, R. B. Order-Order Morphological Transitions for Dual Stimulus Responsive Diblock Copolymer Vesicles. *Macromolecules* **2016**, *49*, 1016−1025.
(64) Blanazs, A.; Verber, R.; Mykhaylyk, O. O.; Ryan, A. J.; Heath, J. Z.; Douglas, C. W. I.; Armes, S. P. Sterilizable Gels from Thermoresponsive Block Copolymer Worms. *J. Am. Chem. Soc.* **2012**, *134*, 9741−9748.
(65) Vogt, A. P.; Sumerlin, B. S. Temperature and Redox Responsive Hydrogels from ABA Triblock Copolymers Prepared by RAFT Polymerization. *Soft Matter* **2009**, *5*, 2347−2351.
(66) Lovett, J. R.; Warren, N. J.; Ratcliffe, L. P. D.; Kocik, M. K.; Armes, S. P. pH-Responsive Non-Ionic Diblock Copolymers: Ionization of Carboxylic Acid End-Groups Induces an Order-Order Morphological Transition. *Angew. Chem., Int. Ed.* **2015**, *54*, 1279−1283.
(67) Derry, M. J.; Fielding, L. A.; Warren, N. J.; Mable, C. J.; Smith, A. J.; Mykhaylyk, O. O.; Armes, S. P. In Situ Small-Angle X-Ray Scattering Studies of Sterically-Stabilized Diblock Copolymer Nanoparticles Formed During Polymerization-Induced Self-Assembly in Non-Polar Media. *Chem. Sci.* **2016**, *7*, 5078−5090.
(68) Thompson, K. L.; Mable, C. J.; Cockram, A.; Warren, N. J.; Cunningham, V. J.; Jones, E. R.; Verber, R.; Armes, S. P. Are Block Copolymer Worms More Effective Pickering Emulsifiers than Block Copolymer Spheres? *Soft Matter* **2014**, *10*, 8615−8626.
(69) Thompson, K. L.; Chambon, P.; Verber, R.; Armes, S. P. Can Polymersomes Form Colloidosomes? *J. Am. Chem. Soc.* **2012**, *134*, 12450−12453.
(70) Sugihara, S.; Armes, S. P.; Blanazs, A.; Lewis, A. L. Non-Spherical Morphologies from Cross-Linked Biomimetic Diblock Copolymers Using RAFT Aqueous Dispersion Polymerization. *Soft Matter* **2011**, *7*, 10787−10793.
(71) Skrabania, K.; Miasnikova, A.; Bivigou-Koumba, A. M.; Zehm, D.; Laschewsky, A. Examining the UV-Vis Absorption of RAFT Chain Transfer Agents and Their Use for Polymer Analysis. *Polym. Chem.* **2011**, *2*, 2074−2083.
(72) Chiefari, J.; Chong, Y. K. B.; Ercole, F.; Krstina, J.; Jeffery, J.; Le, T. P. T.; Mayadunne, R. T. A.; Meijs, G. F.; Moad, C. L.; Moad, G.; Rizzardo, E.; Thang, S. H. Living Free-Radical Polymerization by Reversible Addition-Fragmentation Chain Transfer: The RAFT Process. *Macromolecules* **1998**, *31*, 5559−5562.

DOI: 10.1021/acs.macromol.6b02643
Macromolecules 2017, 50, 1482−1493

(73) Moad, G.; Rizzardo, E.; Thang, S. H. Living Radical Polymerization by the RAFT Process-A Second Update. *Aust. J. Chem.* **2009**, *62*, 1402−1472.
(74) Moad, G.; Rizzardo, E.; Thang, S. H. Radical Addition-Fragmentation Chemistry in Polymer Synthesis. *Polymer* **2008**, *49*, 1079−1131.
(75) Warren, N. J.; Mykhaylyk, O. O.; Mahmood, D.; Ryan, A. J.; Armes, S. P. RAFT Aqueous Dispersion Polymerization Yields Poly(ethylene Glycol)-Based Diblock Copolymer Nano-Objects with Predictable Single Phase Morphologies. *J. Am. Chem. Soc.* **2014**, *136*, 1023−1033.
(76) Verber, R.; Blanazs, A.; Armes, S. P. Rheological Studies of Thermo-Responsive Diblock Copolymer Worm Gels. *Soft Matter* **2012**, *8*, 9915−9922.
(77) Li, Y.; Armes, S. P. Synthesis of Model Primary Amine-Based Branched Copolymers by Pseudo-Living Radical Copolymerization and Post-Polymerization Coupling of Homopolymers. *Macromolecules* **2009**, *42*, 939−945.
(78) Li, Y.; Ryan, A. J.; Armes, S. P. Synthesis of Well-Defined Branched Copolymers by Quaternization of Near-Monodisperse Homopolymers. *Macromolecules* **2008**, *41*, 5577−5581.
(79) Rosselgong, J.; Armes, S. P. Quantification of Intramolecular Cyclization in Branched Copolymers by ^{1}H NMR Spectroscopy. *Macromolecules* **2012**, *45*, 2731−2737.
(80) Lovett, J. R.; Ratcliffe, L. P. D.; Warren, N. J.; Armes, S. P.; Smallridge, M. J.; Cracknell, R. B.; Saunders, B. R. A Robust Cross-Linking Strategy for Block Copolymer Worms Prepared via Polymerization-Induced Self-Assembly. *Macromolecules* **2016**, *49*, 2928−2941.
(81) Won, Y.-Y.; Davis, H. T.; Bates, F. S. Giant Wormlike Rubber Micelles. *Science* **1999**, *283*, 960−963.

DOI: 10.1021/acs.macromol.6b02643
Macromolecules 2017, 50, 1482−1493